

Ferroptosis-Related Long Noncoding RNA Signature Predicts Prognosis of Clear Cell Renal Carcinoma

(clear cell renal carcinoma / ferroptosis / long noncoding RNA / prognosis / biomarker)

J. W. LIU, F. SUPANDI, S. K. DHILLON

Institute of Biological Sciences, Faculty of Science, University Malaya, Kuala Lumpur, Malaysia

Abstract. Clear cell renal cell carcinoma (ccRCC) is very common and accounts for most kidney cancer deaths. While many studies are being conducted in finding the prognostic signatures of ccRCC, we believe that ferroptosis, which involves programmed cell death dependent on iron accumulation, has therapeutic potential in ccRCC. Recent research has shown that long noncoding RNAs (lncRNAs) are involved in ferroptosis-related tumour processes and are closely related to survival in patients with ccRCC. Hence, in this study we aim to further explore the role of ferroptosis-related lncRNAs (FRLs) in ccRCC, hoping to establish a signature to predict the survival outcome of ccRCC. We analysed transcriptome data from The Cancer Genome Atlas database (TCGA) and ferroptosis-related genes (FRGs) from FerrDb to identify FRLs using Pearson's correlation. Lasso Cox regression analysis and multivariate Cox proportional hazards models screened seventeen optimal FRLs for developing prognostic signatures. Kaplan-Meier survival curves and ROC curves were then plotted for validating the sensitivity, specificity, and accuracy of the identified signatures. Gene Set Enrichment Analysis and CIBERSORT algorithm were deployed to explore the role of these FRLs in the tumour microenvironment. It was concluded that these models demonstrate excellent performance in

predicting prognosis among patients with ccRCC, also indicating association with the clinicopathologic parameters such as tumour grade, tumour stage and tumour immune infiltration. In conclusion, our findings provide novel insights into ferroptosis-related lncRNAs in ccRCC, which are important targets for investigating the tumorigenesis of ccRCC.

Introduction

According to Sung et al. (2021), there were 431,288 new diagnostic cases and 179,368 deaths in renal cell carcinoma (RCC) all over the world in 2020. Excess body weight, tobacco use and hypertension are the major established risk factors for developing RCC (American Cancer Society, 2021). Although several therapeutic options such as surgery, partial nephrectomy, radical nephrectomy, targeted therapies and immunotherapy are available (Hsieh et al., 2017), the 5-year survival rate is only 13 % if RCC has spread to a distant part of the body (American Cancer Society, 2021). One of the most common RCC is ccRCC, which is responsible for approximately 70–75 % of all renal cell carcinoma cases (Störkel et al., 1997). In clinical practice, the most significant indicator of prognosis and treatment of ccRCC is tumour stage. However, the same tumour stage has been shown to yield different outcomes in patients based on molecular heterogeneity (Ljungberg et al., 2015; Motzer et al., 2015). Hence, it is crucial and urgent to identify individualized biomarkers that can help to predict survival in patients. This will also help in the identification of patients that are at a greater risk of death.

There are three types of cancer cell death, apoptosis, autophagy and necrosis, during the tumour treatment (Lu et al., 2018). Recently, ferroptosis, a new type of cell death that is dependent on excessive iron accumulation and lipid peroxidation, has been identified. In ferroptosis, the level of intracellular accumulation of reactive oxygen species (ROS) exceeds the cell's anti-oxidation capacity (Yu et al., 2017). The concept of ferroptosis was first proposed by Dixon et al. in 2012. Due to its importance in cell death, recent studies have begun to unravel the role of ferroptosis genes in cancer survival and cell death. Interestingly, p53, a key tumour suppress-

Received August 8, 2021. Accepted January 7, 2022.

Corresponding author: Assoc. Prof. Dr. Sarinder Kaur Dhillon, Institute of Biological Sciences, Faculty of Science, University of Malaya, 50603 Kuala Lumpur, Malaysia. Phone: (+60)379676741; e-mail: sarinder@um.edu.my

Abbreviations: ccRCC – clear cell renal cell carcinoma, DELs – differentially expressed lncRNAs, FRGs – ferroptosis-related genes, FRLs – ferroptosis-related lncRNAs, KEGG – Kyoto Encyclopaedia of Genes and Genomes, Lasso – least absolute shrinkage and selection operator, lncRNA – long noncoding RNA, OS – overall survival, RCC – renal cell carcinoma, ROC – receiver operating characteristic, ROS – reactive oxygen species, TCGA – The Cancer Genome Atlas, TME – tumour microenvironment.

sor that contains homozygous mutations in ~50–60 % of human cancers, has been reported to induce ferroptosis (Jiang et al., 2015; Baugh et al., 2018). It was also reported that ferroptosis could potentially contribute to the tumour-suppressive activity of p53 (Jiang et al., 2015). Sensitivity profiling in 177 cancer cell lines showed that GPX4 is the key ferroptosis regulator in diffusing large B-cell lymphomas and renal cell carcinomas (Yang et al., 2014). A recent study on ferroptosis by Li et al. (2020a) indicated that ferroptosis played important roles in pancreatic cancer, hepatocellular carcinoma, gastric cancer, colorectal cancer, breast cancer, lung cancer, and clear cell renal cell carcinoma. Another study by Eling et al. (2015) demonstrated that artesunate (ART) induces ROS production and stimulates ferroptosis in pancreatic ductal adenocarcinoma cell lines. Based on the aforementioned studies, it is very likely that ferroptosis may offer potential therapeutic options in tumour therapy. Evidence also shows that a number of ferroptosis inducers can effectively kill tumour cells in various preclinical animal experiments (Hassannia et al., 2019; Stockwell and Jiang, 2020). Hence, ferroptosis-inducing agents show potential as novel therapeutics for the tumour treatments. A recent study discovered that immunotherapy-activated CD8⁺ T cells enhanced the ferroptosis-specific lipid peroxidation in cancer cells, and in turn, the increase of ferroptosis-specific lipid peroxidation was essential in enhancing the immunotherapy efficacy (Wang et al., 2019b). Therefore, the mechanism of T cell-stimulated tumour ferroptosis may provide a new therapeutic approach for treating cancer.

Long noncoding RNAs are defined as RNAs longer than 200 nucleotides that could mediate gene regulation through binding with DNA, RNA, or proteins and are correlated to tumour progression, recurrence, and metastasis (Hauptman and Glavač, 2013). LncRNAs function as fundamental regulators, participating in chromatin organization, transcription, post-translational regulation (Choudhari et al., 2020) and regulation of signalling pathways including p53, NF- κ B, PI3K/AKT and Notch (Peng et al., 2017). The following studies have reported the role of lncRNA in regulating ferroptosis. A study by Wang et al. (2019a) demonstrated that LINC00336 serves as a competing endogenous RNA to inhibit ferroptosis in lung cancer. Lu et al. (2020) revealed that lncRNA PVT1 regulated ferroptosis via miR-214/TFR1/TP53 axis. Similarly, a study by Ma et al. (2021) proved that silencing lncRNA MEG8 induces ferroptosis and inhibits proliferation of haemangioma endothelial cells by regulating the miR497-5P/NOTCH2 pathway. To date, what is not yet clear is the impact of ferroptosis-related lncRNAs (FRLs) from sequence data on the overall survival in ccRCC patients.

In this study, we aimed to develop a FRL signature for predicting prognosis of ccRCC patients and explore its role in the tumour microenvironment (TME).

Material and Methods

Data collection

The level 3 RNA-Seq transcriptome data of patients with ccRCC and clinically relevant data were downloaded from the TCGA GDC data portal (<https://portal.gdc.cancer.gov/>). The data comprised 539 tumour patients and 72 normal samples. Patients with incomplete recording of clinical information were excluded. After data cleaning, 501 patients were selected for further analysis. The clinical characteristics of patients are displayed in Table S1.

The Genome Reference Consortium Human Build 38 (GRCh38) annotation file for long noncoding RNA was derived from the GENCODE website (<https://www.genecodegenes.org/human/>). In the TCGA dataset, we identified 14,086 lncRNAs according to the Ensemble IDs. In addition, 259 ferroptosis-related genes (Driver: 108; suppressor: 69; marker: 111) were obtained from FerrDb (Zhou and Bao, 2020), a database that provides comprehensive information on ferroptosis regulators and markers and ferroptosis-disease associations. Immune infiltration data was derived from CIBERSORT (Newman et al., 2015), which includes 22 types of tumour-infiltrating immune cells, as mentioned in Zhang et al. (2021).

Identification of ferroptosis-related lncRNAs

The limma package (Ritchie et al., 2015) was adopted for recognizing significant differentially expressed ferroptosis-related genes (FRGs) and differentially expressed lncRNAs (DELs) between ccRCC tissues and healthy tissues according to log₂FC. Subsequently, biological pathways associated with FRGs were assessed using the “clusterProfiler” package (Yu et al., 2012) to investigate Gene Ontology (GO) and Kyoto Encyclopaedia of Genes and Genomes (KEGG), with the inclusion criteria of P value < 0.05 and q value < 0.05.

Co-expression analysis was then performed between FRGs and DELs based on Pearson’s correlation analysis. Following the study by Liang et al. (2021), a cut-off of Pearson’s correlation coefficient > 0.3 and P value < 0.001 for lncRNA was perceived as FRLs.

Development and validation of the ferroptosis-related lncRNA prognostic signature

We first screened prognosis-related lncRNAs (P value < 0.001) by univariate Cox regression analysis. The 501 patients were first randomly stratified into training and validation (1st validation) sets at a ratio of 5 : 5 using the “caret” package (Kuhn, 2020). Subsequently, these 501 patients were randomly divided into two validation sets (2nd and 3rd validation cohorts at a ratio of 7 : 3). The training and validation datasets were used for constructing and testing the FRL-related prognostic risk signature, respectively. All the FRLs were used in the subsequent least absolute shrinkage and selection operator (Lasso) analysis. After filtering by Lasso analysis, a risk model from the selected lncRNAs was constructed

by multivariate Cox proportional hazards model. The coefficients obtained from multivariate Cox proportional hazards model were utilized to produce the following risk score (RS) equation: $RS = \text{coefficient } a \times \text{expression level of lncRNA } a + \text{coefficient } b \times \text{expression level of lncRNA } b + \dots + \text{coefficient } n \times \text{expression level of lncRNA } n$. Based on this equation, the RS per ccRCC patient was independently calculated in the training and validation datasets. Finally, the ccRCC patients were assigned to high- and low-risk groups by the median value of the RS.

Kaplan-Meier survival curves were used to assess the predictive power of the FRLs using the “survival” package (Therneau and Grambsch, 2000) and “survminer” (Kassambara et al., 2021) package. To evaluate the predictive accuracy of the FRLs, receiver operating characteristic (ROC) curve and area under the ROC curve (AUC) were computed by the “survivalROC” package (Heagerty and Saha-Chaudhuri, 2013). Uni- and multivariate analysis were implemented to verify the independent prognostic factor. A nomogram was further established by package “rms” (Harrell, 2021) for prediction of the probable 1-, 3-, and 5-year survival of the ccRCC patients.

Gene set enrichment and statistical analysis

Gene set enrichment analysis (GSEA) (version 4.0.1, <http://www.broadinstitute.org/gsea>) was carried out to identify the lncRNA signature in KEGG by using gene sets of “c2.cp.kegg.v7.4.symbols.gmt”. Gene dataset permutations were set to 1,000 for each analysis, whereas statistical significance was set at $P < 0.05$ and false discovery rate (FDR) $q < 0.25$. To further examine the effect of the signature on the TME of ccRCC, we estimated the immune infiltrate level between high- and low-risk groups.

All statistical analyses were performed with R software (version 4.0.5, <http://www.R-project.org>). The Wilcoxon signed-rank test was used to identify differential tumour-infiltrating immune cells, whereas Pearson’s correlation test was used to identify FRLs.

Results

Enrichment analysis of ferroptosis-related genes

According to the criteria of $|\log_2FC| > 1$ and $FDR < 0.05$, we found 77 FRGs (37 up-regulated and 40 down-regulated) (Table S2). Through the KEGG analysis, the FRGs were mainly involved in the HIF-1 signaling pathway, microRNA in cancer, ferroptosis, PD-L1 expression and PD-1 checkpoint pathway in cancer, IL-17 signalling pathway, renal cell carcinoma, pancreatic cancer, and bladder cancer (Fig. 1A; Table S3). Biological Process (BP) regulated the response to oxidative stress, cellular response to chemical stress and reactive oxygen species metabolic process. Cellular Component (CC) mainly participated in the apical part of the cell, organelle outer membrane and basolateral plasma mem-

brane. Molecular Function (MF) was enriched in iron ion binding, ferric iron binding and oxidoreductase activity, acting on NAD(P)H (Fig. 1B; Table S3).

Ferroptosis-related lncRNAs in ccRCC

By setting the cut-off of $|\log_2FC| > 2$ and $FDR < 0.05$, 956 DELs were uncovered. These DELs were displayed in the volcano plot via package “ggplot2” (Wickham, 2016) (Fig. 2). Among these FRGs and DELs, 688 FRLs were confirmed by co-expression analysis (Pearson’s correlation coefficient > 0.3 and $P \text{ value} < 0.001$) (Fig. S1).

Construction of ferroptosis-related lncRNA signature

Univariate Cox regression analysis was employed for FRLs, and the result showed that 140 lncRNAs were significantly associated with the overall survival (OS) of ccRCC ($P < 0.001$) (Fig. S2). Lasso regression analysis and multi-Cox proportional hazards model were run on these 140 lncRNAs in the training cohort to further explore the prognostic predictive effect of the lncRNA in ccRCC patients. Initially, the lncRNA expression data was merged with the survival data of each patient. The baseline clinicopathological features of the training cohort and three validation cohorts were summarized in Table 1A and Table 1B, separately. There is no statistical difference in clinical characteristics (age, gender, grade, stage) among the different cohorts, with $P > 0.05$. The prognostic risk signature was established using the training dataset and was validated using three validation datasets. The Lasso regression analysis was first utilized to identify the most significant lncRNAs by selecting the optimal penalty parameter λ correlated with the minimum 10-fold cross-validation (Fig. 3A, B). The multivariate Cox regression model further yielded 17 optimal prognostic FRLs (Fig. 3C). Among them, 10 lncRNAs (AC008742.1, AC010980.2, AC011700.1, AC084876.1, AC090337.1, AC139491.2, LINC01271, MANCR, PRKAR1B-AS1, TMEM246-AS1) are risk factors, seven lncRNAs (AC004066.1, AC005722.3, AC007406.3, AC093583.1, AL928921.1, LINC02073, PSORS1C3) are protective factors, as shown in the Sankey diagram (Fig. 3D), which revealed the association between prognostic FRLs, ferroptosis-related genes, and risk types. The RS equation was calculated as: $RS = (-0.1779 \times AL928921.1 \text{ expression}) + (0.1840 \times AC011700.1 \text{ expression}) + (0.1974 \times AC008742.1 \text{ expression}) - (0.2883 \times AC007406.3 \text{ expression}) + (0.1428 \times AC090337.1 \text{ expression}) + (0.2899 \times LINC01271 \text{ expression}) - (0.2070 \times AC005722.3 \text{ expression}) + (0.2169 \times PRKAR1B-AS1 \text{ expression}) - (0.1990 \times AC004066.1 \text{ expression}) + (0.1480 \times MANCR \text{ expression}) - (0.1458 \times AC093583.1 \text{ expression}) - (0.1822 \times PSORS1C3 \text{ expression}) + (0.3154 \times AC084876.1 \text{ expression}) + (0.1754 \times AC010980.2 \text{ expression}) - (0.1401 \times LINC02073 \text{ expression}) + (0.1127 \times AC139491.2 \text{ expression}) + (0.3129 \times TMEM246-AS1 \text{ expression})$. As shown in Fig. 4, the distribution of the

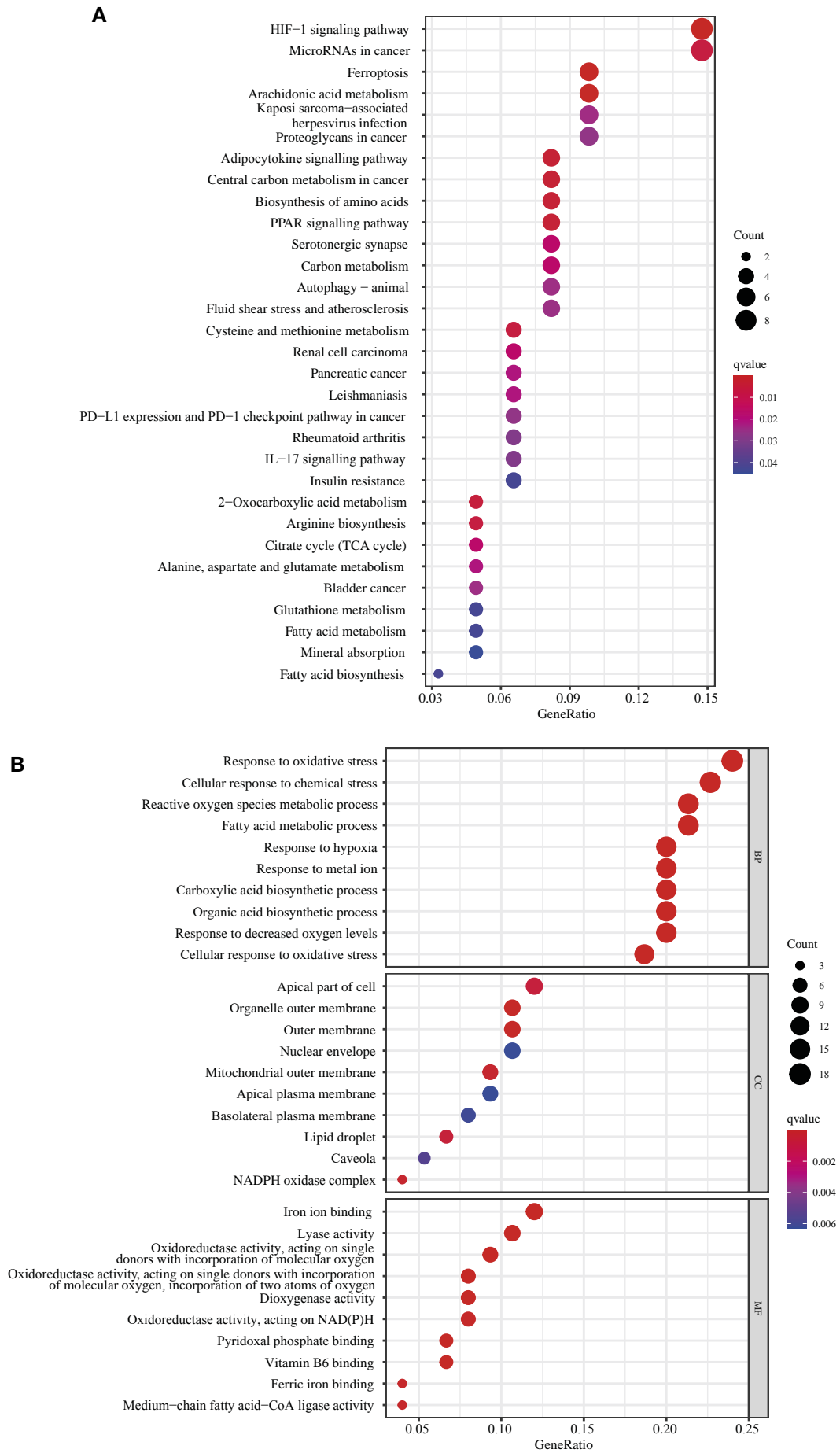


Fig. 1. KEGG and GO analysis for FRGs. (A) KEGG and (B) GO.

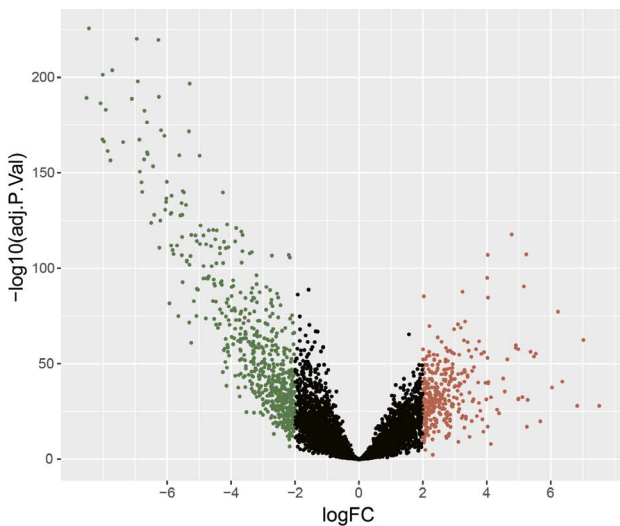


Fig. 2. Volcano plots displaying the differentially expressed lncRNAs between ccRCC and normal tissue samples, where up-regulated lncRNAs are represented by red dots, down-regulated by green dots, and black dots represent lncRNAs with insignificant difference.

RS, OS status, and expression profiles of the signature based on 17 FRLs was displayed in the training and validation cohorts. In the training cohort, the high-risk

groups had evidently higher values of the risk score (Fig. 4A) and lower survival rate (Fig. 4B). Moreover, with the risk score increasing, the expression of protective lncRNA (AL928921.1, AC007406.3, AC005722.3, AC004066.1, AC093583.1, PSORS1C3, LINC02073) decreased, whereas that of the risk lncRNA (AC011700.1, AC008742.1, AC090337.1, LINC01271, PRKAR1B-AS1, MANCR, AC084876.1, AC010980.2, AC139491.2, TMEM246-AS1) increased (Fig. 4C). Similar results were obtained in the 1st validation (Fig. 4D, 4E, 4F), 2nd validation (Fig. 4G, 4H, 4I), and 3rd validation (Fig. 4J, 4K, 4L) cohorts.

Validation of the prognostic score

As presented in Fig. 5A to D, the 3- and 5-year survival rates were 0.829 and 0.851, respectively, in the training cohort, and 0.751 and 0.755, respectively, in the 1st validation cohort; the AUCs for the 3- and 5-year survival prediction were 0.751 and 0.755, respectively. A similar trend was found in the 2nd validation cohort (Fig. 5E, F) and 3rd validation cohort (Fig. 5G, H). These results showed that our signature had an excellent performance for the prognosis of patients with ccRCC.

The survival analysis was also performed for the training cohort and validation cohorts. The Kaplan-Meier results in the training cohort revealed poorer survival in the high-risk group than in the low-risk group ($P < 0.001$)

Table 1. Baseline clinicopathological features for the training dataset and 1st validation dataset (A), 2nd validation dataset and 3rd validation dataset (B)

(A)

Covariates	(A)	Total	Test	Train	P value
Age	≤ 65	332 (66.27 %)	103 (69.13 %)	229 (65.06 %)	0.4368
	> 65	169 (33.73 %)	46 (30.87 %)	123 (34.94 %)	
Gender	Female	172 (34.33 %)	49 (32.89 %)	123 (34.94 %)	0.7336
	Male	329 (65.67 %)	100 (67.11 %)	229 (65.06 %)	
Grade	Grade 1–2	228 (45.51 %)	69 (46.31 %)	159 (45.17 %)	0.892
	Grade 3–4	273 (54.49 %)	80 (53.69 %)	193 (54.83 %)	
Stage	Stage I–II	304 (60.68 %)	89 (59.73 %)	215 (61.08 %)	0.8553
	Stage III–IV	197 (39.32 %)	60 (40.27 %)	137 (38.92 %)	

(B)

Covariates	Type	Total	Test	Train	P value
Age	≤ 65	332 (66.27 %)	172 (69.08 %)	160 (63.49 %)	0.2197
	> 65	169 (33.73 %)	77 (30.92 %)	92 (36.51 %)	
Gender	Female	172 (34.33 %)	76 (30.52 %)	96 (38.1 %)	0.0909
	Male	329 (65.67 %)	173 (69.48 %)	156 (61.9 %)	
Grade	Grade 1–2	228 (45.51 %)	115 (46.18 %)	113 (44.84 %)	0.8319
	Grade 3–4	273 (54.49 %)	134 (53.82 %)	139 (55.16 %)	
Stage	Stage I–II	304 (60.68 %)	155 (62.25 %)	149 (59.13 %)	0.5327
	Stage III–IV	197 (39.32 %)	94 (37.75 %)	103 (40.87 %)	

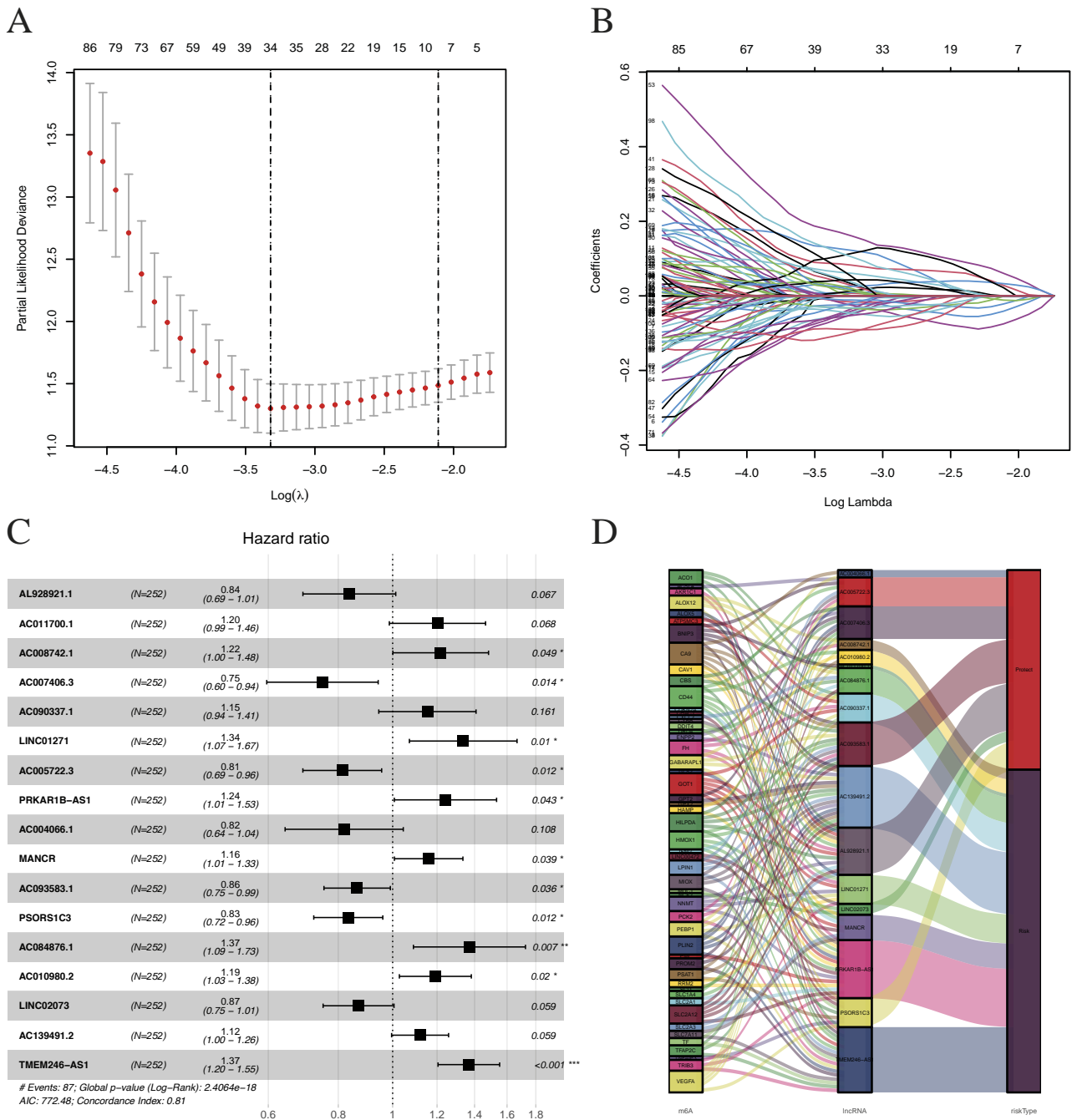


Fig. 3. (A) Partial likelihood deviance for tuning parameter selection in the Lasso analysis in the training dataset. **(B)** Lasso coefficient profiles in the Lasso analysis in the training dataset. **(C)** The hazard ratio (HR) value and its 95% confidence interval with associated P value of the multivariate Cox proportional hazards model were shown in the forest plot. HR > 1 represents high expression of lncRNA unfavourable for prognosis, HR < 1 indicates high expression of lncRNA favourable for prognosis. **(D)** The Sankey diagram showed the association between prognostic FRLs, ferroptosis-related genes, and risk types. An lncRNA linked to red is a protective lncRNA, linked to dark purple represents a risk lncRNA.

(Fig. 5I). Likewise, the same tendency was discovered in the validation cohorts with all P values < 0.001 (1st validation cohort: Fig. 5J; 2nd validation cohort: Fig. 5K; 3rd validation cohort: Fig. 5L). Taken together, the results showed that the RS based on the prognostic risk signature could accurately indicate the prognosis of ccRCC patients.

To determine the prognostic values of RS and various clinicopathological factors in ccRCC, uni- and multivariate Cox regression analyses were performed in each cohort. Univariate analysis indicated that age (P = 0.004), stage (P < 0.001) and risk score (P < 0.001) have a significant effect on OS in the training cohort (Fig. 6A). Subsequently, these factors were also included into

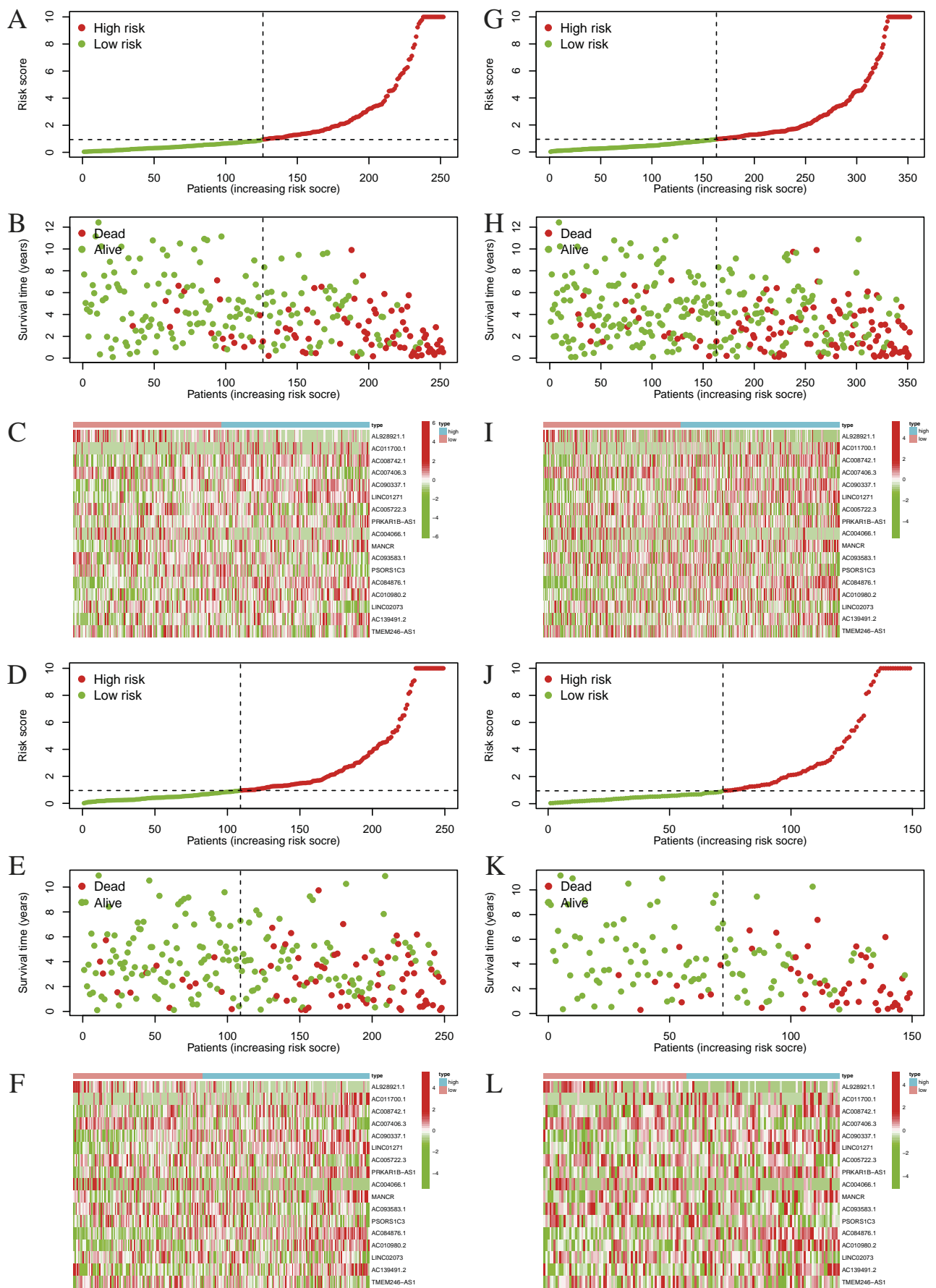


Fig. 4. The RS distribution, survival status, and lncRNA expression in the datasets. (A, B, C) Training cohort, (D, E, F) 1st validation cohort, (G, H, I) 2nd validation cohort, and 3rd validation cohort (J, K, L).

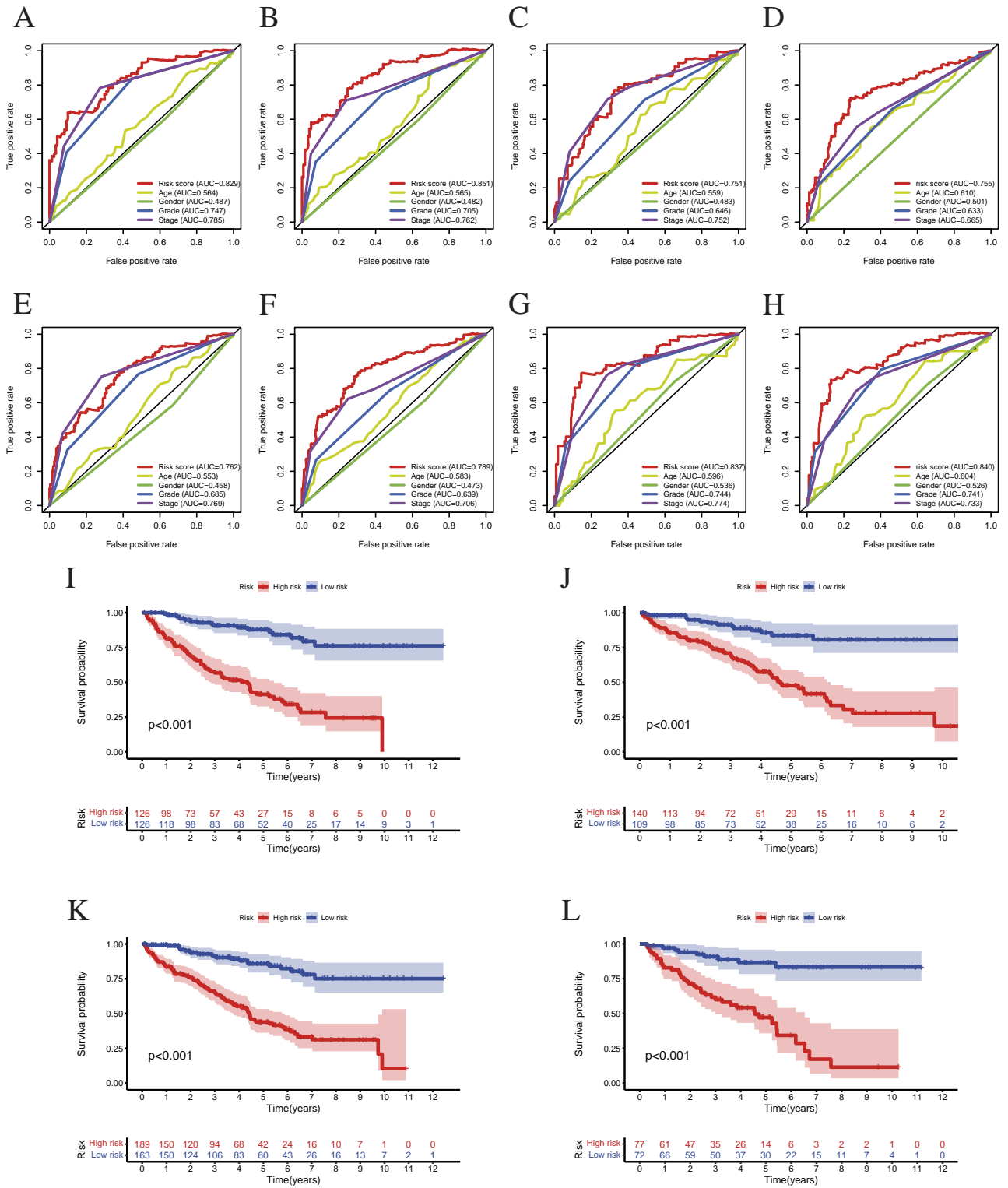


Fig. 5. Kaplan-Meier curves of overall survival for the high-risk and low-risk groups and ROC curves for 3- and 5-year survival for predicting survival in the cohorts. (A, B) ROC for 3- and 5-year survival in the training cohort. (C, D) ROC for 3- and 5-year survival in the 1st validation cohort. (E, F) ROC for 3- and 5-year survival in the 2nd validation cohort. (G, H) ROC for 3- and 5-year survival in the 3rd validation cohort. (I) The training cohort. (J) 1st validation cohort. (K) 2nd validation cohort. (L) 3rd validation cohort.

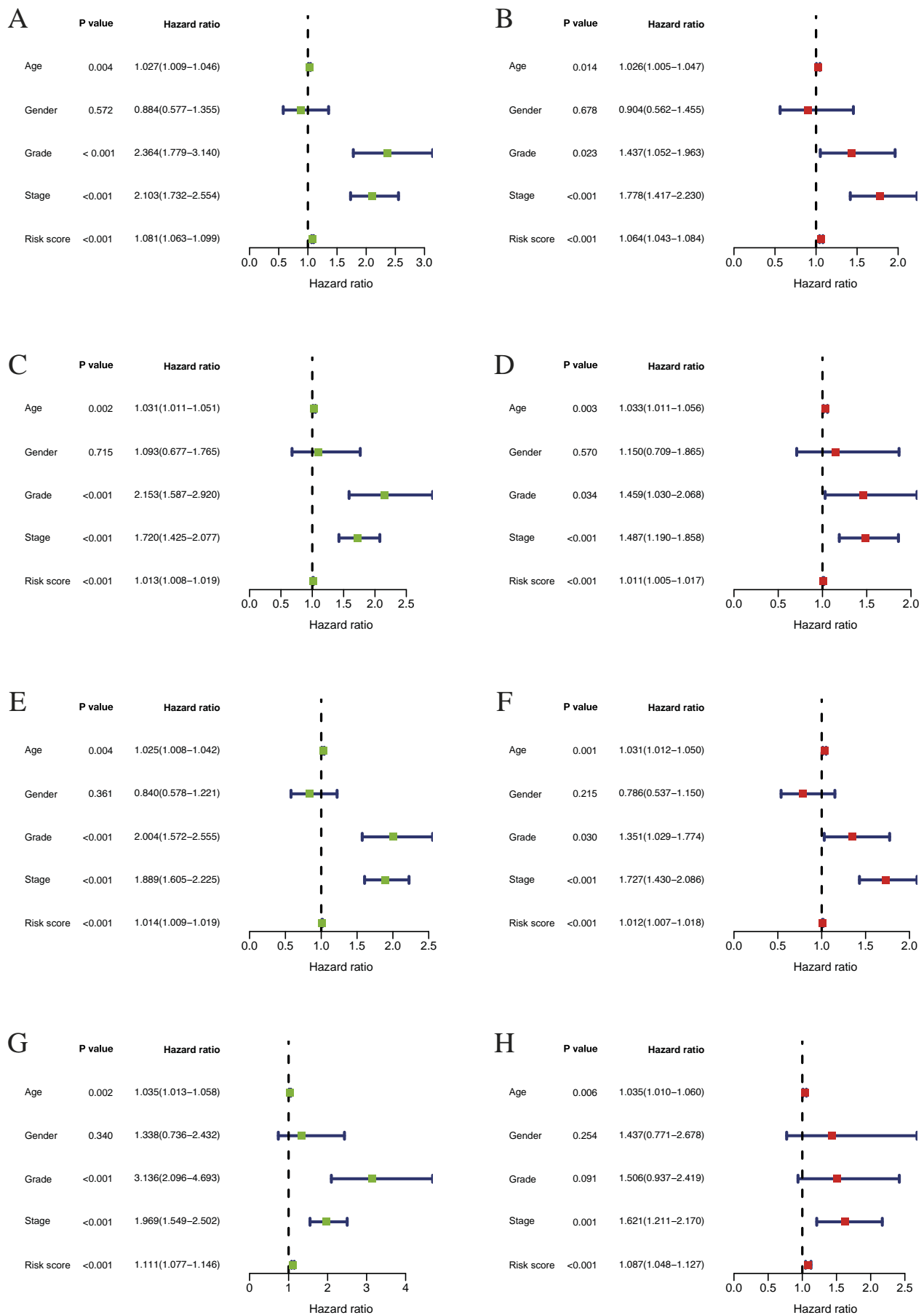


Fig. 6. Forest plots of the uni- and multivariate Cox regression analysis indicated that RS, age and stage were independent risk factors for OS in the training cohort (A, B), 1st validation cohort (C, D), 2nd validation cohort (E, F) and 3rd validation cohort (G, H).

multivariate Cox regression analysis, which further confirmed age ($P = 0.014$), stage ($P < 0.001$) and risk score ($P < 0.001$) as independent prognostic factors (Fig. 6B). Simultaneously, the same tendency was acquired in the three validation cohorts (Fig. 6C–H).

Nomogram establishment and clinical value of the RS

To study the 1-, 3-, and 5-year prognosis of the patients with ccRCC, a nomogram was plotted using the training dataset by integrating the independent prognostic factors (age, stage, risk score) (Fig. 7A). Interestingly, the same tendency was acquired in the validation dataset (Fig. S3). Using the nomogram, the 1-, 3-, and 5-year

survival rates could be predicted by the corresponding value of total points based on the independent prognostic factors (Zhang et al., 2021).

We further explored the relationships among ten risk lncRNAs (AC011700.1, AC008742.1, AC090337.1, LINC01271, PRKAR1B-AS1, MANCR, AC084876.1, AC010980.2, AC139491.2, TMEM246-AS1), RS, and clinicopathological features (age, gender, grade, stage) (Table 2). The RS was found distinctly higher in advanced-stage tumours and higher grade tumours (Fig. 7B, C). The same tendency was acquired in the validation cohorts (Table S4, Fig. S4). These findings demonstrate that the risk score based on our signature can also reflect tumour progression.

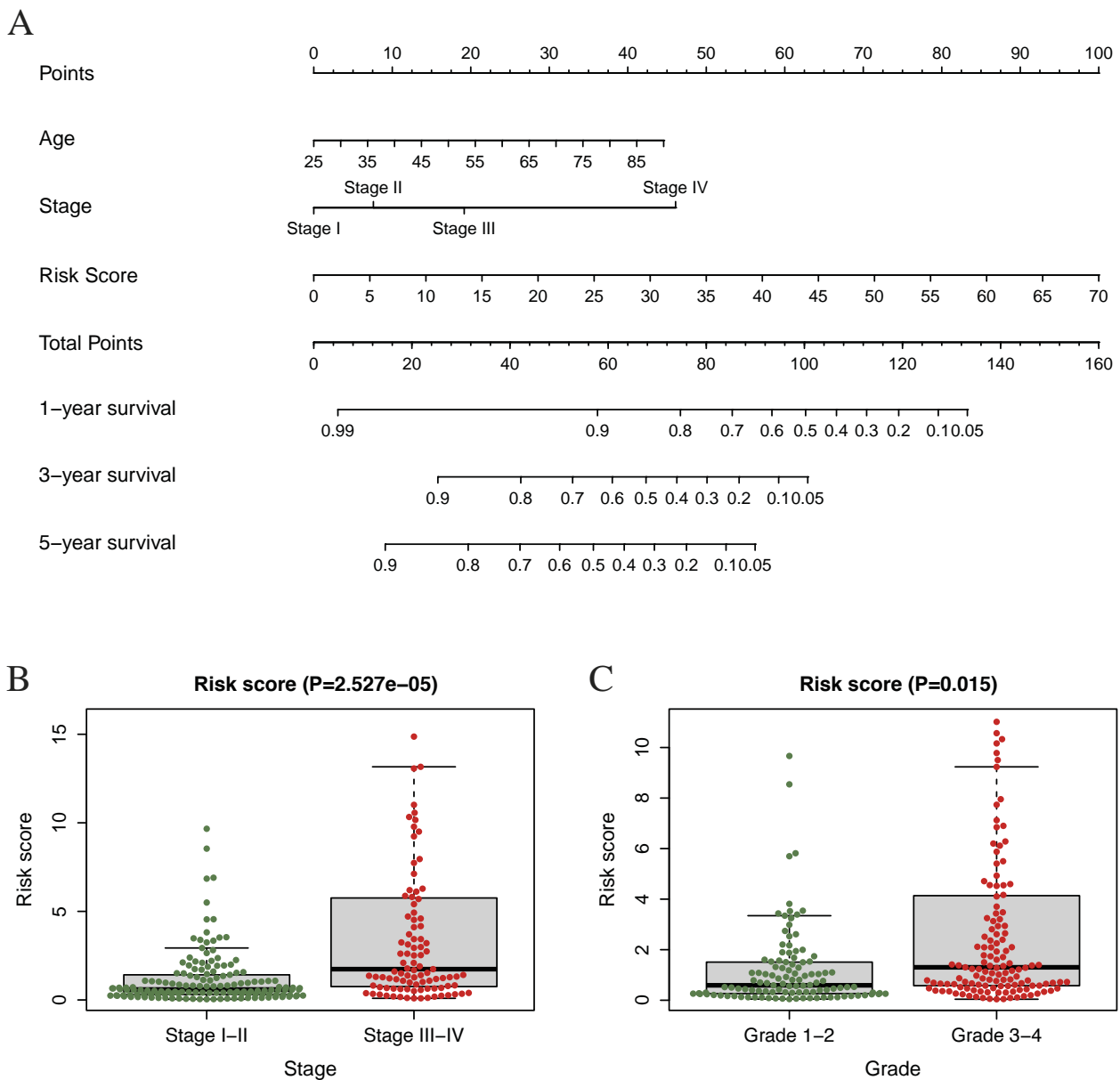


Fig. 7. (A) A nomogram plot was built to qualify risk assessment for ccRCC patients. (B) Relationships between the risk score and tumour stage in ccRCC. (C) Relationships between the risk score and tumour grade in ccRCC.

Table 2. Association of the RS and risk genes with clinical factors in ccRCC

LncRNA	Age (≤ 65 / > 65)	Gender (Female / Male)	Grade (1 and 2 / 3 and 4)	Stage (I–II / III–IV)
AC011700.1	–1 (0.318)	–0.862 (0.390)	–0.629 (0.530)	–0.551 (0.582)
AC008742.1	0.199 (0.843)	1.234 (0.219)	–0.789 (0.431)	–1.755 (0.081)
AC090337.1	–0.237 (0.813)	1.013 (0.312)	–0.032 (0.975)	–2.74 (0.007)
LINC01271	–0.249 (0.804)	–0.286 (0.775)	–3.26 (0.001)	–3.99 (8.877e-05)
PRKAR1B-AS1	–0.493 (0.623)	–2.477 (0.014)	–0.819 (0.414)	–4.076 (6.363e-05)
MANCR	0.424 (0.672)	–2.868 (0.005)	–2.277 (0.024)	–3.134 (0.002)
AC084876.1	–1.76 (0.080)	1.475 (0.141)	–3.03 (0.003)	–2.891 (0.004)
AC010980.2	–0.904 (0.367)	0.592 (0.555)	–3.871 (1.384e-04)	–3.893 (1.388e-04)
AC139491.2	–0.867 (0.387)	–1.227 (0.221)	–1.338 (0.182)	–1.111 (0.268)
TMEM246-AS1	–0.353 (0.725)	3.613 (3.908e-04)	1.825 (0.069)	1.325 (0.186)
Risk Score	–1.366 (0.174)	0.828 (0.409)	–2.46 (0.015)	–4.407 (2.527e-05)

Description of the important variables in Table 2:

Grade	Grade is the description of a tumour based on how abnormal the tumour cells and the tumour tissue look. It is an indicator of how quickly a tumour is likely to grow and spread.
Stage	Stage refers to the size and/or extent (reach) of the original (primary) tumour and whether or not cancer cells have spread in the body.

To further explore the prognostic value of the 17 lncRNAs, the Kaplan-Meier curve was plotted to confirm the relationship between these lncRNAs and OS. In our analysis, a total of 11 of the 17 lncRNAs (LINC01271, AC010980.2, AC011700.1, MANCR, AC008742.1, AC084876.1, AC090337.1, AC093583.1, LINC02073, AL928921.1, AC004066.1) were identified. The results indicated that the 11 ferroptosis-related lncRNAs were correlated to the OS in ccRCC patients (Fig. 8).

We also evaluated the relationship between the RS and immune cell infiltration. At first, to investigate the tumour immune microenvironment in the patients with ccRCC, the immune landscape of all samples was plotted (Fig. 9A). Next, the numbers of immune cells that showed a significant difference between the low- and high-risk groups were identified. Ten types of immune cells were identified with differences in infiltration between the two groups, namely, plasma cells, T cells follicular helper, Tregs, monocytes, macrophages M0, dendritic cells resting, dendritic cells activated, mast cells resting, mast cells activated, eosinophils (Fig. 9B).

Gene set enrichment analysis

GSEA software was utilized to investigate the Kyoto Encyclopedia of Genes and Genomes (KEGG) to further explore the potential biological behaviour of our signature in patients with ccRCC. The KEGG results revealed that our prognostic signature regulated cancer-related pathways and immune-related pathways such as the pathways in cancer, RCC, NSCLC, mTOR signalling pathways, Wnt signalling pathway, MAPK signalling pathways in low-risk groups (Fig. S5, Table S5).

Discussion

For decades, the diagnosis and treatment of ccRCC patients has been based on clinicopathological factors (Ljungberg et al., 2015; Motzer et al., 2015). While patients may have similar clinical characteristics, the therapeutic effect and their prognosis has a massive gap. Hence, in this study, we explored the various techniques available in data science to predict prognosis of ccRCC using FRLs as potential biomarkers. To the best of our knowledge, this is the first study that attempted to predict prognosis signatures of ccRCC based on FRLs.

This study was inspired by Lu et al. (2018), who highlighted the importance of further research in ferroptosis and its mechanism with regard to the diagnosis and prognosis of cancer. As mentioned before, ferroptosis has been known to be involved in the progression of ccRCC (Li et al., 2020a). This is confirmed in our study, which revealed 77 differentially expressed ferroptosis-related genes. KEGG further revealed that most of the FRGs participated in the HIF-1 signalling pathway, microRNA in cancer, ferroptosis, PD-L1 expression and PD-1 checkpoint pathway in cancer, IL-17 signalling pathway, RCC, prostatic cancer, and breast cancer. A recent study by Li et al. (2020b) demonstrated that the achievement of FG-4592 (an inhibitor of prolyl hydroxylase of HIF) pre-treatment is mainly based on decreasing ferroptosis at the early stage of FA-induced kidney injury via Akt/GSK-3 β -mediated Nrf2 activation. Tang et al. (2020) reported that the IL-17 signalling pathway is a potential target affected by erastin (ferroptosis inducer), which indicated that the ferroptosis inducer eras-

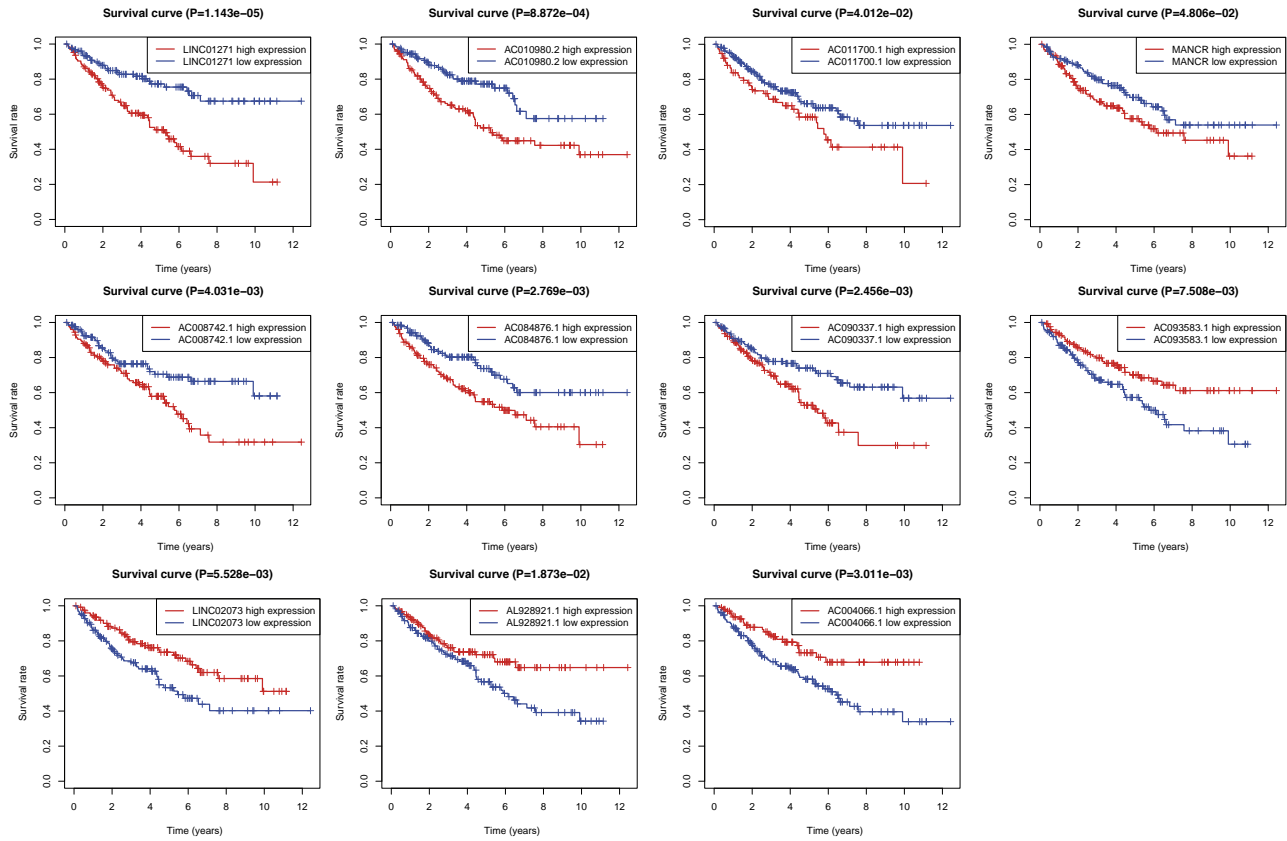


Fig.8. Validation of the prognostic value of 17 ferroptosis-related lncRNAs in ccRCC by Kaplan-Meier curve.

tin may be regarded as a potential agent for cancer immunotherapy.

Several studies have reported that lncRNAs play diverse roles in cancer (Schmitt and Chang, 2016; Carlevaro-Fita et al., 2020). For example, lncRNA BX357664 regulates cell proliferation through regulating the TGF- β 1/p38/HSP27 axis in RCC (Liu et al., 2016). lncRNA SNHG11 facilitates tumour metastasis by interacting with and stabilizing HIF-1 α (Xu et al., 2020). lncRNA HANR promotes tumorigenesis in hepatocellular carcinoma (Xiao et al., 2017). In this study, we identified 956 DELs in ccRCC. In accordance with the present results, our studies demonstrated that lncRNAs are strongly associated with the malignancy in ccRCC. Moreover, lncRNAs have been reported to have important roles in ferroptosis. Mao et al. (2018) illustrated that lncRNA P53RRA can directly interact with the functional domain of signalling proteins in the cytoplasm, thereby modulating p53 modulators to suppress cancer progression. Yang et al. (2020) reported that silencing of lncRNA ZFAS1 attenuated ferroptosis by functioning as ceRNA. In our research, we implemented a co-expression analysis among FRGs and DELs, and thus 688 lncRNAs were identified as FRLs. The result showed a strong link between FRGs and FRLs in ccRCC samples, suggesting that FRLs are related to the tumorigenicity of ccRCC.

Seventeen lncRNA out of all FRLs, referring to AC008742.1, AC010980.2, AC011700.1, AC084876.1, AC090337.1, AC139491.2, LINC01271, MANCR, PRKAR1B-AS1, TMEM246-AS1, AC004066.1, AC005722.3, AC007406.3, AC093583.1, AL928921.1, LINC02073, PSORS1C3, were associated with prognosis independently and hence were used as the prognostic signature. ROC curves (AUC at 3 years: 0.829; AUC at 5 years: 0.851) in the training cohort and in three validation datasets with similar results confirmed excellent specificity and sensitivity of our prognostic signature. Survival curves with P value < 0.001 in each dataset exhibited good efficacy of our signatures in stratifying patients into high and low risk of mortality. Univariate and multivariate Cox analysis further demonstrated that age, stage and risk score were independent prognostic factors. We also verified the effect of our risk score in the patients with the same tumour stage, and we could see that the risk score of stage III–IV was obviously higher than in stage I–II. All the analyses show that our ferroptosis-related lncRNA signature may be a beneficial supplement for better stratifying patients and for providing a more individualized treatment method. We further integrated three independent prognostic factors (age, stage, risk score) to develop a nomogram for calculating points that could reflect survival.

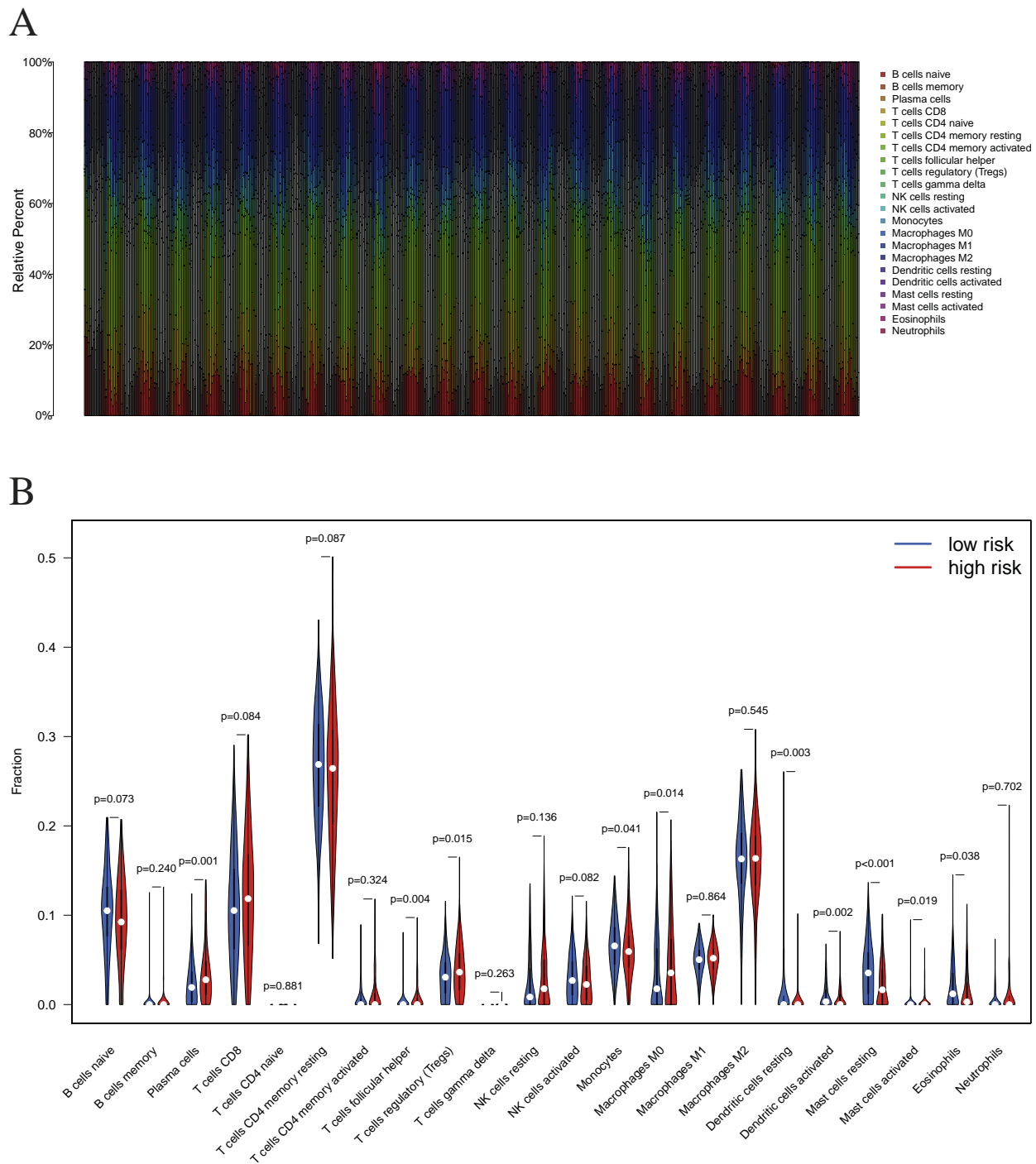


Fig. 9. (A) The immune landscape of all ccRCC patients included in this study. **(B)** Relationships between the risk score and the immune cell infiltration in ccRCC patients.

Ferroptosis either promoted or suppressed tumour progression, with release of multiple signalling molecules depending on the damage-associated molecular patterns and activation of the immune response triggered by ferroptotic damage within the tumour microenvironment (Jiang et al., 2020; Chen et al., 2021). We investigated GSEA to elucidate the potential biological mechanisms of our signature in the TME. We found that several immune-related pathways were enriched in the

low-risk group. Increasing studies support the involvement of lncRNAs in the complicated tumour-stromal crosstalk and stimulation of tumour microenvironments (Zhou et al., 2020). To explore the TME in patients with ccRCC, we plotted the immune landscape for all samples. Indeed, we made a comparison of the infiltration level of 22 immune cell types between the high- and low-risk groups. Plasma cells, T cells follicular helper, T cells regulatory (Tregs), monocytes, macrophages M0,

dendritic cells resting, dendritic cells activated, mast cells resting, mast cells activated, and eosinophils were identified to be differentially infiltrated in ccRCC. These results supported the implication of our risk signature in the ccRCC microenvironment and provided valuable reference for immunotherapy.

Undeniably, there are limitations in our study. Data on the patients in our study were obtained only from TCGA, hence we could not perform any validation. Our findings need to be tested by multicentre cohorts in the clinical domain.

Conclusion

In conclusion, this study scientifically assessed the prognostic value, role in the tumour immune microenvironment, and regulatory mechanisms of 17 ferroptosis-related lncRNA-based signature in patients with ccRCC. It brought novel insights into ferroptosis-related lncRNAs in ccRCC, which are important targets for investigating the tumorigenesis of ccRCC. Their further analyses could lead to development of personalized and individualized treatment strategies.

Contribution of authors

Sarinder Kaur Dhillon and Jia Wen Liu designed the study. Jiawen Liu performed the analysis. Farahaniza Binti Supandi helped in gene enrichment analysis. All authors contributed to the writing of the manuscript.

Supplementary Material

Supplementary Material for this manuscript can be downloaded from <http://sarinderkaur.com/SupplementaryMaterial.pdf>

References

- American Cancer Society (2021) *Cancer Facts and Figures 2021*.
- Baugh, E. H., Ke, H., Levine, A. J., Bonneau, R. A., Chan, C. S. (2018) Why are there hotspot mutations in the TP53 gene in human cancers? *Cell Death Differ.* **25**, 154-160.
- Carlevaro-Fita, J., Lanzós, A., Feuerbach, L., Hong, C., Mas-Ponte, D., Pedersen, J. S.; PCAWG Drivers and Functional Interpretation Group, Johnson, R.; PCAWG Consortium (2020) Cancer lncRNA Census reveals evidence for deep functional conservation of long noncoding RNAs in tumorigenesis. *Commun. Biol.* **3**, 56.
- Chen, X., Kang, R., Kroemer, G., Tang, D. (2021) Broadening horizons: the role of ferroptosis in cancer. *Nature Rev. Clin. Oncol.* **18**, 280-296.
- Choudhari, R., Sedano, M. J., Harrison, A. L., Subramani, R., Lin, K. Y., Ramos, E. I., Lakshmanaswamy, R., Gadad, S. S. (2020) Long noncoding RNAs in cancer: From discovery to therapeutic targets. *Adv. Clin. Chem.* **95**, 105-147.
- Dixon, S. J., Lemberg, K. M., Lamprecht, M. R., Skouta, R., Zaitsev, E. M., Gleason, C. E., Patel, D. N., Bauer, A. J., Cantley, A. M., Yang, W. S., Morrison, B., 3rd, Stockwell, B. R. (2012) Ferroptosis: an iron-dependent form of nonapoptotic cell death. *Cell* **149**, 1060-1072.
- Eling, N., Reuter, L., Hazin, J., Hamacher-Brady, A., Brady, N. R. (2015) Identification of artesunate as a specific activator of ferroptosis in pancreatic cancer cells. *Oncoscience* **2**, 517-532.
- Harrell, F. E. Jr. (2021) rms: Regression Modeling Strategies. Retrieved from <https://CRAN.R-project.org/package=rms>.
- Hassannia, B., Vandenabeele, P., Vanden Berghe, T. (2019) Targeting ferroptosis to iron out cancer. *Cancer Cell* **35**, 830-849.
- Hauptman, N., Glavač, D. (2013) Long non-coding RNA in cancer. *Int. J. Mol. Sci.* **14**, 4655-4669.
- Heagerty, P. J., Saha-Chaudhuri, P. (2013) survivalROC: Time-dependent ROC curve estimation from censored survival data. Retrieved from <https://CRAN.R-project.org/package=survivalROC>
- Hsieh, J. J., Purdue, M. P., Signoretti, S., Swanton, C., Albiges, L., Schmidinger, M., Heng, D. Y., Larkin, J., Ficarra, V. (2017) Renal cell carcinoma. *Nature Rev. Dis. Primers* **3**, 17009.
- Jiang, L., Kon, N., Li, T., Wang, S. J., Su, T., Hibshoosh, H., Baer, R., Gu, W. (2015) Ferroptosis as a p53-mediated activity during tumour suppression. *Nature* **520**, 57-62.
- Jiang, M., Qiao, M., Zhao, C., Deng, J., Li, X., Zhou, C. (2020) Targeting ferroptosis for cancer therapy: exploring novel strategies from its mechanisms and role in cancers. *Transl. Lung Cancer Res.* **9**, 1569-1584.
- Kassambara, A., Kosinski, M., Biecek, P. (2021) survminer: Drawing Survival Curves using 'ggplot2'. Retrieved from <https://CRAN.R-project.org/package=survminer>
- Kuhn, M. (2020) caret: Classification and Regression Training. Retrieved from <https://CRAN.R-project.org/package=caret>
- Li, J., Cao, F., Yin, H.-L., Huang, Z.-J., Lin, Z.-T., Mao, N., Sun, B., Wang, G. (2020a) Ferroptosis: past, present and future. *Cell Death Dis.* **11**, 88.
- Li, X., Zou, Y., Xing, J., Fu, Y.-Y., Wang, K.-Y., Wan, P.-Z., Zhai, X.-Y. (2020b) Pretreatment with roxadustat (FG-4592) attenuates folic acid-induced kidney injury through anti-ferroptosis via Akt/GSK-3 β /Nrf2 pathway. *Oxid. Med. Cell. Longev.* **2020**, 6286984.
- Liang, J., Zhi, Y., Deng, W., Zhou, W., Li, X., Cai, Z., Zhu, Z., Zeng, J., Wu, W., Dong, Y., Huang, J., Zhang, Y., Xu, S., Feng, Y., Ding, F., Zhang, J. (2021) Development and validation of ferroptosis-related lncRNAs signature for hepatocellular carcinoma. *PeerJ* **9**, e11627.
- Liu, Y., Qian, J., Li, X., Chen, W., Xu, A., Zhao, K., Hua, Y., Huang, Z., Zhang, J., Liang, C., Su, S., Li, P., Shao, P., Li, J., Qin, C., Wang, Z. (2016) Long noncoding RNA BX357664 regulates cell proliferation and epithelial-to-mesenchymal transition via inhibition of TGF- β 1/p38/HSP27 signaling in renal cell carcinoma. *Oncotarget* **7**, 81410-81422.
- Ljungberg, B., Bensalah, K., Canfield, S., Dabestani, S., Hofmann, F., Hora, M., Kuczyk, M. A., Lam, T., Marconi, L., Merseburger, A. S., Mulders, P., Powles, T., Staehler, M., Volpe, A., Bex, A. (2015) EAU guidelines on renal cell carcinoma: 2014 update. *Eur. Urol.* **67**, 913-924.

- Lu, B., Chen, X. B., Ying, M. D., He, Q. J., Cao, J., Yang, B. (2018) The role of ferroptosis in cancer development and treatment response. *Front. Pharmacol.* **8**, 992-992.
- Lu, J., Xu, F., Lu, H. (2020) lncRNA PVT1 regulates ferroptosis through miR-214-mediated TFR1 and p53. *Life Sci.* **260**, 118305.
- Ma, Q., Dai, X., Lu, W., Qu, X., Liu, N., and Zhu, C. (2021) Silencing long non-coding RNA MEG8 inhibits the proliferation and induces the ferroptosis of hemangioma endothelial cells by regulating miR-497-5p/NOTCH2 axis. *Biochem. Biophys. Res. Commun.* **556**, 72-78.
- Mao, C., Wang, X., Liu, Y., Wang, M., Yan, B., Jiang, Y., Shi, Y., Shen, Y., Liu, X., Lai, W., Yang, R., Xiao, D., Cheng, Y., Liu, S., Zhou, H., Cao, Y., Yu, W., Muegge, K., Yu, H., Tao, Y. (2018) A G3BP1-interacting lncRNA promotes ferroptosis and apoptosis in cancer via nuclear sequestration of p53. *Cancer Res.* **78**, 3484-3496.
- Motzer, R. J., Jonasch, E., Agarwal, N., Beard, C., Bhayani, S., Bolger, G. B., Chang, S. S., Choueiri, T. K., Costello, B. A., Derweesh, I. H., Gupta, S., Hancock, S. L., Kim, J. J., Kuzel, T. M., Lam, E. T., Lau, C., Levine, E. G., Lin, D. W., Michaelson, M. D., Olencki, T., Pili, R., Plimack, E. R., Rampersaud, E. N., Redman, B. G., Ryan, C. J., Sheinfeld, J., Shuch, B., Sircar, K., Somer, B., Wilder, R. B., Dwyer, M., Kumar, R. (2015) Kidney cancer, version 3.2015. *J. Natl. Compr. Canc. Netw.* **13**, 151-159.
- Newman, A. M., Liu, C. L., Green, M. R., Gentles, A. J., Feng, W., Xu, Y., Hoang, C. D., Diehn, M., Alizadeh, A. A. (2015) Robust enumeration of cell subsets from tissue expression profiles. *Nat. Methods* **12**, 453-457.
- Peng, W. X., Koirala, P., Mo, Y. Y. (2017) lncRNA-mediated regulation of cell signaling in cancer. *Oncogene* **36**, 5661-5667.
- Ritchie, M. E., Phipson, B., Wu, D., Hu, Y., Law, C. W., Shi, W., Smyth, G. K. (2015) limma powers differential expression analyses for RNA-sequencing and microarray studies. *Nucleic Acids Res.* **43**, e47.
- Schmitt, A. M., Chang, H. Y. (2016) Long noncoding RNAs in cancer pathways. *Cancer Cell* **29**, 452-463.
- Stockwell, B. R., Jiang, X. (2020) The chemistry and biology of ferroptosis. *Cell Chem. Biol.* **27**, 365-375.
- Störkel, S., Eble, J. N., Adlakha, K., Amin, M., Blute, M. L., Bostwick, D. G., Darson, M., Delahunt, B., Iczkowski, K. (1997) Classification of renal cell carcinoma: Workgroup No. 1. Union Internationale Contre le Cancer (UICC) and the American Joint Committee on Cancer (AJCC). *Cancer* **80**, 987-989.
- Sung, H., Ferlay, J., Siegel, R. L., Laversanne, M., Soerjomataram, I., Jemal, A., Bray, F. (2021) Global cancer statistics 2020: GLOBOCAN estimates of incidence and mortality worldwide for 36 cancers in 185 countries. *CA Cancer J. Clin.* **71**, 209-249.
- Tang, B., Zhu, J., Li, J., Fan, K., Gao, Y., Cheng, S., Kong, C., Zheng, L., Wu, F., Weng, Q., Lu, C., Ji, J. (2020) The ferroptosis and iron-metabolism signature robustly predicts clinical diagnosis, prognosis and immune microenvironment for hepatocellular carcinoma. *Cell Commun. Signal.* **18**, 174.
- Therneau, T. M., Grambsch, P. M. (2000) *Modeling Survival Data: Extending the Cox Model*. Springer-Verlag, New York.
- Wang, M., Mao, C., Ouyang, L., Liu, Y., Lai, W., Liu, N., Shi, Y., Chen, L., Xiao, D., Yu, F., Wang, X., Zhou, H., Cao, Y., Liu, S., Yan, Q., Tao, Y., Zhang, B. (2019a) Long noncoding RNA LINC00336 inhibits ferroptosis in lung cancer by functioning as a competing endogenous RNA. *Cell Death Differ.* **26**, 2329-2343.
- Wang, W., Green, M., Choi, J. E., Gijón, M., Kennedy, P. D., Johnson, J. K., Liao, P., Lang, X., Kryczek, I., Sell, A., Xia, H., Zhou, J., Li, G., Li, J., Li, W., Wei, S., Vatan, L., Zhang, H., Szeliga, W., Gu, W., Liu, R., Lawrence, T. S., Lamb, C., Tanno, Y., Cieslik, M., Stone, E., Georgiou, G., Chan, T. A., Chinnaiyan, A., Zou, W. (2019b) CD8+ T cells regulate tumour ferroptosis during cancer immunotherapy. *Nature* **569**, 270-274.
- Wickham, H. (2016) *ggplot2: Elegant Graphics for Data Analysis*. Springer-Verlag, New York.
- Xiao, J., Lv, Y., Jin, F., Liu, Y., Ma, Y., Xiong, Y., Liu, L., Zhang, S., Sun, Y., Tipoe, G. L., Hong, A., Xing, F., Wang, X. (2017) lncRNA HANR promotes tumorigenesis and increase of chemoresistance in hepatocellular carcinoma. *Cell. Physiol. Biochem.* **43**, 1926-1938.
- Xu, L., Huan, L., Guo, T., Wu, Y., Liu, Y., Wang, Q., Huang, S., Xu, Y., Liang, L., He, X. (2020) lncRNA SNHG11 facilitates tumor metastasis by interacting with and stabilizing HIF-1 α . *Oncogene* **39**, 7005-7018.
- Yang, W. S., SriRamaratnam, R., Welsch, M. E., Shimada, K., Skouta, R., Viswanathan, V. S., Cheah, J. H., Clemons, P. A., Shamji, A. F., Clish, C. B., Brown, L. M., Girotti, A. W., Cornish, V. W., Schreiber, S. L., Stockwell, B. R. (2014) Regulation of ferroptotic cancer cell death by GPX4. *Cell* **156**, 317-331.
- Yang, Y., Tai, W., Lu, N., Li, T., Liu, Y., Wu, W., Li, Z., Pu, L., Zhao, X., Zhang, T., Dong, Z. (2020) lncRNA ZFAS1 promotes lung fibroblast-to-myofibroblast transition and ferroptosis via functioning as a ceRNA through miR-150-5p/SLC38A1 axis. *Aging (Albany NY)* **12**, 9085-9102.
- Yu, G., Wang, L.-G., Han, Y., He, Q.-Y. (2012) clusterProfiler: an R package for comparing biological themes among gene clusters. *OMICS* **16**, 284-287.
- Yu, H., Guo, P., Xie, X., Wang, Y., Chen, G. (2017) Ferroptosis, a new form of cell death, and its relationships with tumourous diseases. *J. Cell. Mol. Med.* **21**, 648-657.
- Zhang, H., Qin, C., Liu, H. W., Guo, X., Gan, H. (2021) An effective hypoxia-related long non-coding RNAs assessment model for prognosis of clear cell renal carcinoma. *Front. Oncol.* **11**, 616722.
- Zhou, L., Zhu, Y., Sun, D., Zhang, Q. (2020) Emerging roles of long non-coding RNAs in the tumor microenvironment. *Int. J. Biol. Sci.* **16**, 2094-2103.
- Zhou, N., Bao, J. (2020) FerrDb: a manually curated resource for regulators and markers of ferroptosis and ferroptosis-disease associations. *Database (Oxford)* **2020**, baaa021.